# FIRE HAZARD CALCULATIONS IN TUNNELS USING CFD

Fathi Tarada


## ABSTRACT

This paper reports on the use of hazard models for fires in tunnels and other enclosed spaces. These hazard models provide important inputs to Computational Fluid Dynamics (CFD) codes, and also facilitate the interpretation of the computed results. The hazard models considered here include models for the chemical composition of the fire load, the fire growth rate, the reduction of visibility due to smoke and the toxicity of combustion gases. These models are therefore important tools for the application of CFD in the assessment of fire risks to passengers in enclosed spaces.


## 1 INTRODUCTION

The use of CFD as a tool to predict airflows in tunnel systems is rapidly gaining world-wide acceptance by health and safety executives, railway authorities, civil engineering contractors and engineering consultants. When CFD is rationally applied by experts for the design of an emergency ventilation system, substantial civil and mechanical/electrical cost savings can be made, while simultaneously offering a high degree of safety to underground passengers. This is due to the deeper insights that CFD offers us with respect to smoke movement and the effect of imposed ventilation.

In order to enjoy the full benefits that CFD has to offer, it is imperative that it is deeply imbedded in a project's design phase, and not just employed as an after-thought. Fig. 1 (after Barry, 1995) outlines a rational strategy of risk assessment and amelioration. Of the seven distinct risk assessment steps proposed in Fig. 1, CFD offers benefits in the 'consequence assessment' step, by allowing us to estimate the rate of development of the hazardous environment, and the subsequent vulnerability of passengers.

A key to the effective use of CFD within a tunnel environment is the careful validation of the CFD models with respect to full-scale fire tests (e.g. Eureka 1995 , Memorial Tunnel 1995) and simple correlations (e.g. for the critical velocity to overcome backlayering). The required grid parameters and model constants developed in the validation phase can then be used for the calculations of a similar tunnel system of interest.

Another important consideration for the effective use of CFD in risk assessment is the provision of reliable inputs to model the hazards (e.g. fire growth rate), and the interpretation of the results in terms of possible risks to passengers. The inputs to a CFD analysis determine its quality, given a well-validated programme and an adequate mesh density. The subsequent interpretation of the results is central to the usefulness of the results. These fundamental issues are the prime concern of this paper.

Fig, 2 gives an overview of the prime inputs and outputs of a CFD-supported hazard analysis of a given fire scenario. The shaded inputs and outputs are considered in this paper. Some of the available models in the literature are presented and compared, and their impact on the safe design of tunnels is discussed.

2nd International Conference on Fire Safety in Enclosed Spaces, 8-9 June 1998, Geneva.

## 2 NOMENCLATURE

| Symbol | Meaning | Units |
|---|---|---|
| $C_i$ | Mass concentration of product 'i' | % |
| D | Optical density | - |
| $D_o$ | Smoke potential | ob.m³/kg |
| $E_{tot}$ | Total combustible energy content of fuel | J |
| $f_i$ | Normalised yield of combustion product 'i' | - |
| F | $= n_{CO}/n_{CO2}$, describing combustion completeness | - |
| FED | Fractional Effective Dose | - |
| $\dot{Q}$ | Total heat release rate | W |
| $k_i$ | maximum yield of product 'i' | g/g |
| K | Specific absorption area | $m^2/kg$ |
| $LCt_{50}$ | Toxic potency | $g.min/m^3$ |
| $\dot{m}_c$ | Rate of fuel mass loss | kg/s |
| $M_i$ | Molecular weight of product 'i' | g/mole |
| n,m,o | Number of carbon, hydrogen and oxygen atoms | - |
| $n_i$ | Number of atoms of product 'i' | - |
| t | Time | min |
| $\dot{V}$ | Volumetric flowrate of air | $m^3/s$ |
| $X_i$ | Volumetric concentration of product 'i' | % |
| $Y_s$ | Soot load (fraction of solid particles to fuel mass loss) | kg/kg |

**Greek**

| | | |
|---|---|---|
| $\alpha$ | Quadratic heat release rate coefficient | $MW/min^2$ |
| $\beta$ | Exponential heat release rate coefficient | $min^{-1}$ |
| $\chi_c$ | Combustion efficiency | - |
| $\sigma$ | Extinction coefficient | $m^{-1}$ |
| $\Delta H_c$ | Specific heat of combustion | J/kg |

**Subscripts**

| | |
|---|---|
| f | Fuel |
| g | Combustion gases |
| i | Combustion product |
| mix | Mixed conditions |

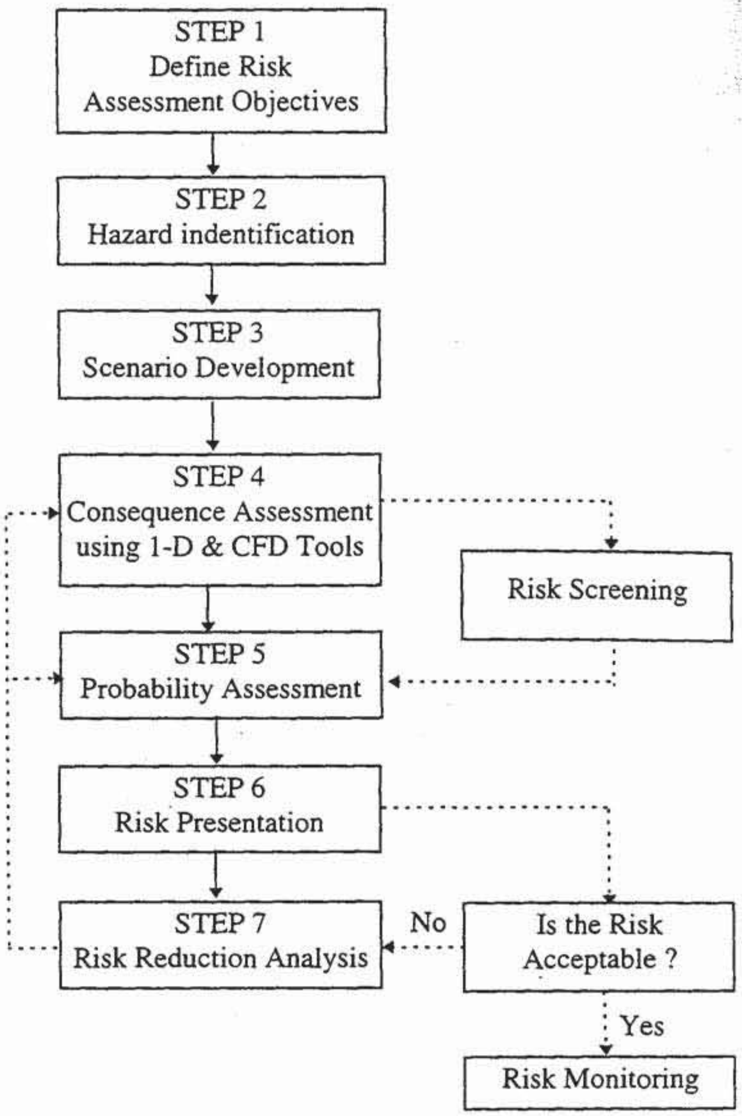


**Fig. 1 : Fire and Explosion Risk Assessment Steps (after Barry, 1995)**

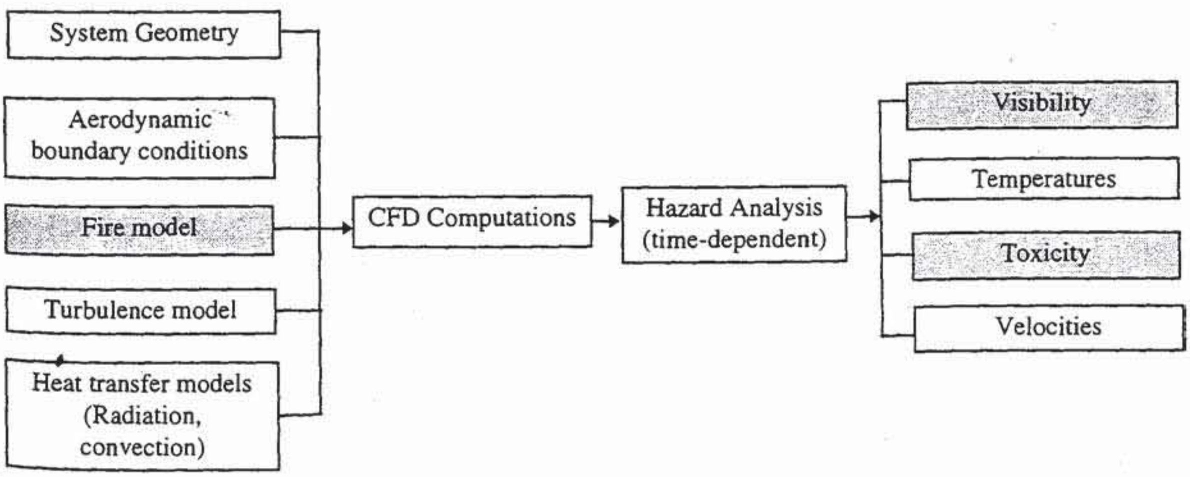


**Fig. 2 : Major Inputs and Outputs from a CFD-supported Hazard Analysis Study**

## 3 FIRE MODEL

### 3.1 Fire Modelling with CFD

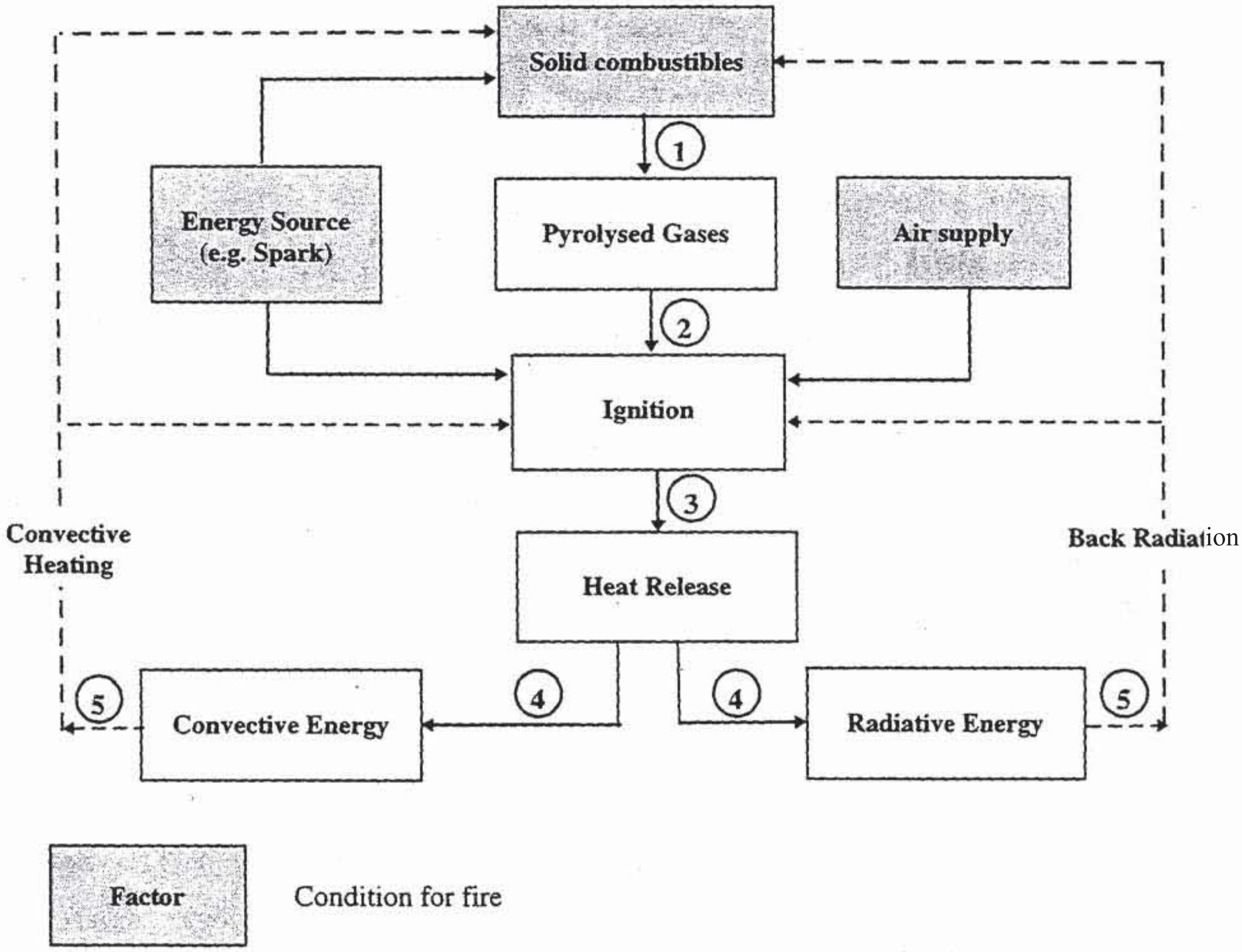


**Fig. 3 : Main Processes in the Ignition and Development of a Fire**

Fig. 3 summarises the main processes in the ignition and development of a fire. In particular, the importance of the simultaneous presence of combustibles, an energy source and an air supply for any fire are underlined.

CFD analyses of fires in tunnels can be conveniently divided into those employing an exothermic combustion model, and those which directly specify the heat release rate.

CFD analyses which include a exothermic combustion model attempt to model the combustion reaction kinetics, such : (Steinert, 1994)

$$(1+F)C_nH_mO_o+\left(\frac{2n+m/2-o}{2}+\frac{n+m/2-o}{2}F\right)O_2 \rightarrow nCO_2+nF.CO+\frac{m}{2}(1+F)H_2O$$

Equation (1)

Calculations undertaken using such combustion models can be thought of as following steps 1 to 4 in Fig. 3 above (e.g. Kumar and Cox, 1985, Tuovinen and Holmstedt, 1994). The heat release rate in such models is related to the specific heat of combustion and the mass flow of the pyrolysed gases, such :

$$\dot{Q} = \chi_c \dot{m}_c \Delta H_c \qquad \text{Equation (2)}$$

where the combustion efficiency, $\chi_c$, is conservatively estimated to be unity.

The majority of CFD analyses of tunnel fires do not model any reaction kinetics, but directly specify a heat release rate at the fire source instead (e.g. Elias et al, 1996). Thus, only step 4 is modelled with this approach. In addition to a heat source, mass sources are introduced to account for, variously, the pyrolysis rate or to obtain a pre-specified flame temperature. Inspite of its apparent simplicity, this approach does have its drawbacks. In particular, it is difficult to combine the requirements for

- A heat release rate that includes both convective and radiative components;
- A well-defined flame temperature (required for assessing radiation hazards, for example);
- Overall mass balance in the system (any mass source introduced has to be balanced by a mass sink, without destroying any smoke layering that may be present);
- Accurate radiative view factors, since fires are typically defined along a surface rather than over a volume in this approach.

None of the current CFD models are sufficiently well developed enough to account for the rate of progress of a fire due to self-ignition (back radiation and convective heating), although great progress in this area has been made in recent years (e.g. Murty Kanury, 1995).

### 3.2 The Definition and Use of Reference Fires

In view of the difficulty in predicting self-ignition and growth in fires, it is important to use the results of full-scale fire tests in calibrating the heat release rates for the fire load under study (e.g. a passenger train). The Eureka fire tests (1995) are particularly useful for calibrating a model or reference fire, defined by simple relationships (Ingason, 1995) :

**Fire growth phase :**

$$Q(t) = \alpha t^2 \qquad 0 \le t \le t_1 \qquad \text{Equation (3)}$$

**Fully developed fire :**

$$Q(t) = Q_{max} \qquad t_1 \le t \le t_2 \qquad \text{Equation (4)}$$

**Fire decay :**

$$Q(t) = Q_{max} \exp(-\beta(t - t_2)) \qquad t > t_2 \qquad \text{Equation (5)}$$

In addition, we can write the condition relating the integral heat release rate to the total combustible energy content of the combustible material, $E_{tot}$ :

$$t_2 = \frac{\chi_c E_{tot}}{Q_{max}} + \frac{2}{3} t_1 - \frac{1}{\beta} \qquad \text{Equation (6)}$$

Fig. 4 shows the measured and reference heat release rates for a fire in an IC train carriage.

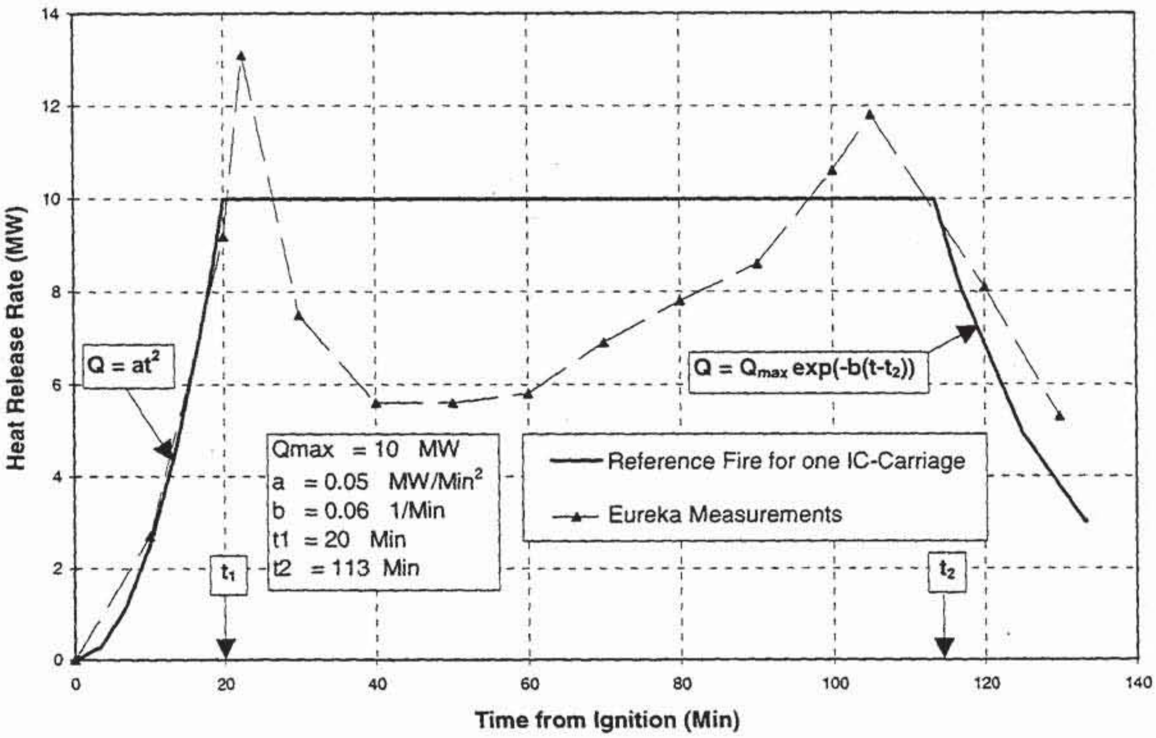


**Fig. 4 : Measured and Reference Fires for an IC Carriage**

Having defined a reference fire for one railway carriage, we may now extrapolate the results for a whole train, assuming linear superposition of the individual reference fires. To do this, we require suitable assumptions for

- The time required for fire spread between carriages. This is likely to be influenced by factors such as the length of flames issuing from a burning carriage, which in turn is influenced by the airflow over the burning carriage (Liew and Deaves, 1998).
- The amount of air available for the fire. If insufficient air is available to feed the fire, retardation of the fire growth rate is likely to occur. As a rule of thumb, 13.4 kJ of heat are released per gramme of oxygen consumed under such ventilation-controlled conditions.

Fig. 5 shows an example of a reference fire for a passenger train comprising ten IC carriages. This example comprises an attempt to rationally extrapolate measured fires from a single carriage to a whole train, and is certainly not without its uncertainties However, only the initial portion of such a reference fire is likely to be relevant to a CFD-supported hazard study, comprising the time elapsed from fire break-out to the incident train stopping, and the subsequent evacuation of passengers.

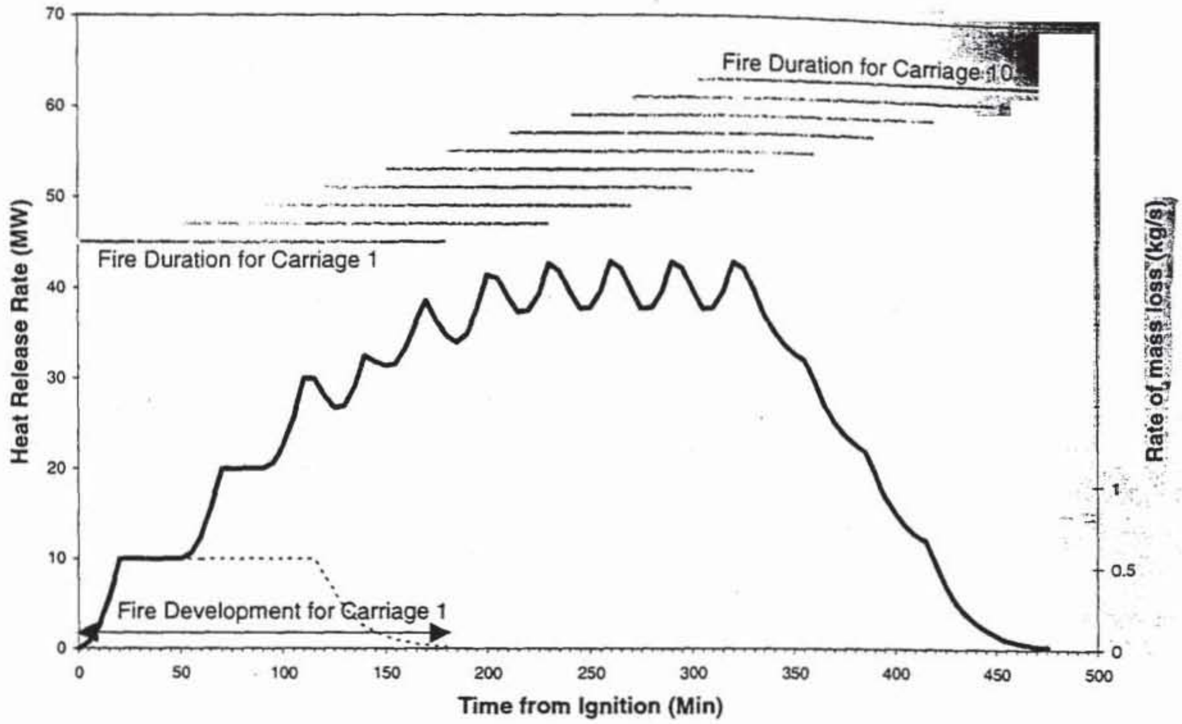


**Fig. 5 : Reference Fire for a Ten-Carriage IC Train**

# 4 HAZARD MODELS

## 4.1 Chemical Composition of Fire Load

The hazard posed by a particular hydrocarbon-based fire load is partially determined by its chemical composition, particularly before flash-over has occurred. The latter can be defined as the explosive-like changeover from a surface to a volumetric fire. In general, the chemical composition of an arbitrary hydrocarbon is described by the number of carbon, hydrogen and oxygen atoms in a single molecule, $C_nH_mO_o$.

The determination of the mean chemical composition of the contents of a train is not simple, especially since the rate of fire progress will be different for the different components, e.g. seats, luggage and paint. The problem can however be simplified for analysing fire tests such as those done by the Eureka project, by calculating the mass-weighted atomic weights for the entire contents of the tested vehicles. Using this technique, we arrive at formulae of $C_{2.3}H_{4.2}O_{1.3}$ and $C_{3.2}H_{4.8}O_{1.7}$ for the Eureka IC and ICE carriages respectively.

It is interesting to observe that the reduction in the total heat load from the older IC carriages to the newer ICE carriages (independently estimated to be 81,067 and 62,480 MJ respectively) is partly negated by the higher carbon content of the fire-resistant materials, which implies higher toxicity (see below).

## 4.2 Estimation of toxicity

Clarke (1997) has suggested the following line of reasoning with respect to post-flashover fires :

- The toxicity of smoke generated in post-flashover fires is dominated by the large amounts of carbon monoxide present.
- In such fires, all organic materials appear to produce roughly the same fraction of carbon monoxide (0.2 kg CO per kg of fuel).
- Therefore, in large fires where carbon monoxide is the dominant toxicant, there is no significant difference in the smoke toxicity of materials.

To enable us to estimate the toxic hazard of a particular scenario, we may use the concept of Fractional Effective Dose, defined by Clarke (1997) such :

$$FED = \frac{exposure \quad dose}{toxic \quad potency \quad (LCt_{50})}$$ Equation (7)

In the above equation, the exposure dose is obtained by integrating the concentration of the toxic product (usually CO) at the victim's location with respect to time. The toxic potency can be estimated as

- $LCt_{50}$ = 200 [g (burnt fuel) . minute / $m^3$ (air)] for disability
- $LCt_{50}$ = 500 [g (burnt fuel) . minute / $m^3$ (air)] for death

In this model, disability or death is assumed to occur when the FED equals unity.

In terms of interpreting CFD results, a time integral of the concentration of the burnt gases is generated at critical locations (e.g. escape routes), and the FED is computed at every time-step.

For more detailed toxicity assessments of a given fire scenario, both in the pre- and post-flashover phases, the volumetric concentration of CO should be estimated at the victim's location. This is given for the toxic product 'i' (where i= CO, $CO_2$, etc.) by Gottuk and Roby (1995) as

$$X_i[\%] = \frac{f_i k_i M_{mix}}{M_i} C_g$$ Equation (8)

where the mass concentration of the combustion gases is approximately given by

$$C_g[\%] = 100 \quad \dot{m}_f / (\dot{m}_a + \dot{m}_f)$$ Equation (9)

In Equation (9), $k_i$ is the maximum theoretical yield in grams of product 'i' per gramme of fuel :

$$k_i = n_i M_i / (n_f M_f)$$ Equation (10)

and the mean molecular weight of the combustion products is given by

$$M_{mix} = \left( \sum_i \frac{C_i / 100}{M_i} \right)^{-1}$$ Equation (11)

The peak normalised yield for carbon monoxide, $f_{CO}$, can be set to 0.2 for ventilation-controlled conditions.

Having estimated the local volumetric concentration of CO, we may then estimate the maximum allowable exposure time using Purser's (1995) relationship for the accumulation of carboxyhaemoglobin :

$$t(X_{CO}) = \frac{30}{8.2925 \times 10^{-4} \left(10^4 X_{CO}\right)^{1.036}} \qquad \text{Equation (12)}$$

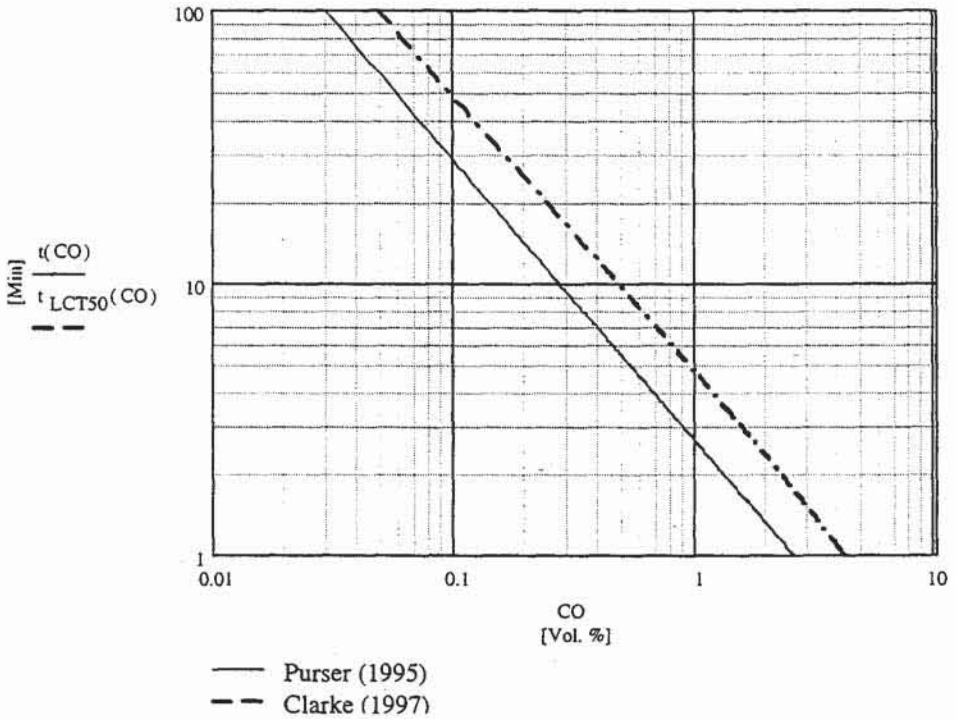


**Fig. 6 : Exposure Times to Disability for an IC Carriage**

Fig. 6 shows a comparison of the maximum exposure times estimated by Clarke's (1997) simplified relationship with Purser's (1995) estimates for ventilation-controlled conditions. Although Clarke's effective dose concept is a useful one, it can be seen from this example that a more detailed knowledge of the chemical composition of the fire load may lead to lower tolerable exposure times.

## 4.3 Estimation of Visibility Limits

In any fire scenario, contamination of the air with airborne solid particles and unburned hydrocarbons leads to a reduction of visibility, and this can significantly impact the chances of escape.

The estimation of visibility is best done using a form of the Discrete Transfer Radiation Method (Carvalho et al, 1991), although this model is currently used only for thermal radiation. For approximate calculations with CFD, a passive tracer gas can be introduced to simulate the spread of fine smoke particles (< 0.1 μm) and unburned hydrocarbons. The spread of larger smoke particles can be estimated using Lagrange particle-tracing methods.

The optical density, D, was defined by Steinert (Eureka, 1995) as the attenuation of the light intensity, I, passing through smoke, such :

$$D = \log_{10}(I_o/I) \qquad \text{Equation (13)}$$

A commonly defined parameter is the extinction coefficient, σ, which is defined such :

$$\sigma = \frac{D}{L}\ln(10) \qquad \text{Equation (14)}$$

Heins (Eureka, 1995) has proposed allowable limits of 1.3 and 0.3 $m^{-1}$ for the optical density and the extinction coefficient respectively. These values correspond to the case when only 5% of the emitted light is received by a light detector that is placed 10 m away.

There are two empirically-based methods to estimate the visibility limits in smoky conditions :

- **The smoke potential method** (Drysdale, 1985) : This proposes that the optical density is linearly related to the mass of pyrolysed gases present in a given volume of air, such :

  $$\frac{D}{L} = \frac{D_o \dot{m}_f}{\dot{V}} \qquad \text{Equation (15)}$$

  The smoke potential $D_o$ has been experimentally derived for many materials, e.g. $D_o$=170 ob.$m^3$/kg for birch plywood.

- **The absorption area method** (Steinert, 1994) : This proposes the following relationship between the extinction coefficient, the specific absorption area K ($m^2$/kg) and the soot load Ys (kg/kg) :

  $$\sigma = \frac{Y_s \dot{m}_f}{\dot{V}} K \qquad \text{Equation (16)}$$

  For unknown hydrocarbons, Steinert recommends the use of the values K=9250 $m^2$/kg and $Y_s$ = 0.04.

Fig. 7 presents a comparison of the results of two methods as a function of smoke concentration. The results are generally in broad agreement for this particular example. In general, the computed results for visibility extents will strongly depend on the smoke properties assumed for the particular CFD simulation.

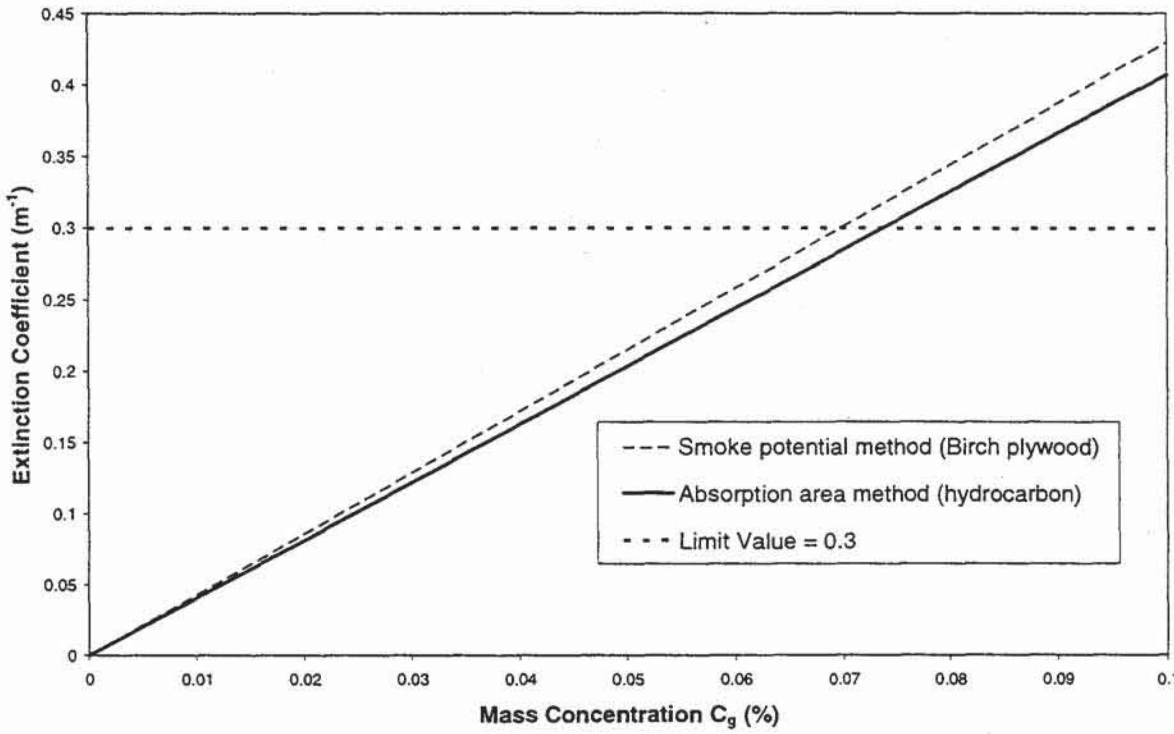


**Fig. 7 : Extinction Coefficients derived from two Visibility Models**

## 5 CONCLUSIONS

A CFD-supported hazard analysis can only be as good as the inputs it receives. This implies careful consideration of the fire model that is implemented in the calculations. In the worst case, false inputs will lead to an unsafe design of emergency ventilation systems and evacuation routes. Therefore, all those involved in the design of vehicle tunnels are well advised to think about the possible size and consequences of fire.

Once the calculations are done, careful interpretation of the results should be carried out using hazard models such as those presented here. This allows maximum benefit to be extracted from the CFD results, by allowing us to realistically model the prevailing conditions during a fire scenario. The insight provided by such simulations can be of significant assistance in

- designing appropriate ventilation systems for smoke management (supply/extract, longitudinal, transverse);
- setting appropriate procedures in case of fire (e.g. evacuation plans, ventilation control, train operation);
- dimensioning critical tunnel geometry parameters (e.g. platform widths, escape passages).

The rational application of CFD to tunnel design therefore offers the potential of significant improvements in the safety of underground passengers.

## 6 REFERENCES

Barry, T.F., 1995, 'An Introduction to Quantitative Risk Assessment in Chemical Process Industries', in The SFPE Handbook of Fire Protection Engineering, 2nd Ed.

Carvalho, M.G., Farias, T. and Fontes, P., 1991, 'Predicting Radiative Heat Transfer in Absorbing, Emitting, and Scattering Media using the Discrete Transfer Method'. In W.A: Fiveland et al, Eds., 'Fundamentals of Radiation Heat Transfer', Vol. 160, pp. 17-26, ASME HTD.

Clarke, F.B., 1997, 'Physiological Effects of Smoke : Managing Escape', ASHRAE Journal, March 1997.

Drysdale, D., 1985, 'An Introduction to Fire Dynamics', John Wiley.

Elias, S.R., Bostwick, P.K. and Raw, M.J., 1996, 'Numerical Simulation of Subway Fires and Ventilation', ASME Fluids Engineering Division Summer Meeting, San Diego, California.

Eureka-Project EU 499 : FIRETUN, Nov. 1995. 'Fires in Transport Tunnels, Report on Full-Scale Tests', Editor : Studiengesellschaft Stahlanwendung e.V., D-40213 Düsseldorf.

Gottuk, D.T. und Roby, R.J., 1995, 'Effect of Combustion Conditions on Species Production', in SFPE Handbook of Fire Protection Engineering.

Ingason, H., 1995, 'Untersuchungsergebnisse zur Energiefreisetzung', Konferenzband zum Brandschutz in Verkehrstunneln, Dresden.

Kumar, S. and Cox, G., 1985, 'Mathematical Modelling of Fires in Road Tunnels', 5th International Symposium on the Aerodynamics and Ventilation of Vehicle Tunnels, Lille, France.

Liew, S. and Deaves, D., 1998, 'Eurotunnel HGV Fire on 18th November 1996 - Fire Development and Effects', Third International Conference on Safety in Road and Rail Tunnels, Nice.

Memorial Tunnel Fire Ventilation Test Program, Nov. 1995. Test Report for Massachusetts Highway Department and Federal Highway Administration.

Murty Kanury, A., 1995, 'Flaming Ignition of Solid Fuels', in The SFPE Handbook of Fire Protection Engineering, 2nd Ed.

Purser, D.A. 1995, 'Toxicity Assessment of Combustion Products', in SFPE Handbook of Fire Protection Engineering.

Steinert, C., 1994, 'Energie und Rauchfreisetzungsraten bei Tunnelbrandversuchen', Tunnel, Vol. 5.

Tuovinen, H. and Holmstedt, G., 1994, 'CFD Modelling of Tunnel Fires', International Conference on Fires in Tunnels, Boras.